MEASUREMENTS AND PREDICTION OF LAMINAR-TURBULENT TRANSITION AT HIGH FREE-STREAM TURBULENCE AND PRESSURE GRADIENTS

Valery Chernoray*, Bercelay Niebles Atencio*, Mohsen Jahanmiri**
***Dept. of Applied Mechanics, Chalmers University of Technology, Göteborg, Sweden,**
****Department of Mechanical and Aerospace Engineering, Shiraz University of Technology, Shiraz, Iran**

Abstract

This paper is focused on measurements and prediction of laminar-turbulent transition at high free-stream turbulence in boundary layers of airfoil geometries with external pressure gradient changeover. Experimental and numerical study is performed for a number of flow cases covering a range of flow Reynolds numbers, turbulence intensities and pressure gradient distributions. The flow parameters in experiments and computations are typical for turbomachinery applications and main motivation of current study is validation of transition models which can be used for transition prediction in such engineering applications. In current work the experimental data are used to validate a transition model by Langtry and Menter which showed good agreement with experiments for all test cases.

1 Introduction

Laminar-turbulent transition has significant importance in aerodynamics by affecting evolution of losses, appearance of separation and stall. The boundary layer state has dominant effect on the distribution of wall shear stress and surface heat transfer. To predict and manage turbulence in different flow cases is beneficial for optimum advantage, namely, to reduce it when it is harmful (e.g. to decrease the skin friction or heat transfer) and to increase it when it is desirable (to avoid flow separation). The prediction of laminar-turbulent transition at high free-stream turbulence is specifically of great importance in turbomachinery where the boundary layer state defines the blade heat transfer and flow separation margins. However it is well-known that prediction of transition is particularly challenging task for turbulence modelling. A number of turbulence models claim possibility of transition prediction and none of them is proven to be flawless so far. A transition model suggested by Menter et al. [1] is based on a correlation-based approach which seems to be able to provide consistent results. This model has been applied to several 2D and 3D test cases by same research group [2] and simulations agreed well with experiments for all test cases at wide range of Reynolds numbers and freestream turbulent intensities. The literature survey shows though that surprisingly few other validation cases of this model are publicly available. To fulfil this gap and to validate applicability of the Langtry and Menter model for turbomachinery applications was the main purpose of current study.

The effect of pressure gradients and turbulence levels on transition was thoroughly investigated by Abu-Ghannam and Shaw [3] who proposed methods to calculate the momentum thickness Reynolds number for the start and the end of the transition zone, defined by them as the region in which the intermittency factor ranges between 0.25 and 0.75.

Walker and Gostelow [4] carried out experiments under high turbulence levels and adverse pressure gradients and found that close to the wall region within the boundary layer, a turbulent pattern was found to be not much affected by the free-stream conditions. The outer part of the boundary layer is more strongly affected by the high turbulence level and pressure gradient. Later, Gostelow et al. [5] found that at strong adverse pressure gradients, the transition occurs quickly but it seems that the velocity profiles do not reflect this before

the transition is completed. In another study, Salomon et al. [6] presented a new method for calculating intermittency in transitional boundary layers with rapidly changing pressure gradients, which is based on experimental studies using the pressure gradient parameter.

Mayle in his well-known paper, [7] mentions some experiments performed by Görtler in 1940 and Liepman in 1943, which analysed the effect of curvature on transition. From the experiments carried out by the latter, the transition Reynolds number depends on the turbulence level and on how strong the curvature is and seems to have a non-negligible effect in low pressure turbines and small engines, where a delay can be found. For compressors, the effects are negligible but still more data and studies are needed. In the same paper, Mayle keeps the discussion regarding the effect of curvature on transition and by using a curvature parameter, analyses its influence on transition Reynolds number.

Other researchers such as Bario and Beral [8] presented the results of their boundary layer measurements on pressure and suction sides of a turbine inlet blade and found on the pressure side that the onset of the transition, for low turbulence levels, occurs when Görtler vortices have been found. On the other hand, for high turbulence levels, the transition occurs at the leading edge of the pressure side. The turbulence effect in the pressure side is considerable compared to that of the suction side. On the suction side, for low turbulence levels, the transition occurs before the flow may get separated and for higher levels of turbulence, the transition moves upstream to the leading edge.

Also, Van Treuren et al. [9] conducted experiments in the suction side of a low pressure inlet turbine for low free stream turbulence level and high free stream turbulence levels. In both cases they worked with low Reynolds numbers (25000 and 50000). At the lowest end of this range, they found strong and steady separation unable to be corrected either increasing the turbulence level or using vortex generator jets. At Reynolds number 50000, strong separation of the flow downstream the suction side of the vane was found for low free stream turbulence levels, but also they found opportunities to reattach the flow by introducing vortex generators and when increasing the turbulence levels.

In spite of the previously mentioned works, more information and study has to be performed in order to understand the effect of the different variables on the transition process over the airfoils, vanes and blades, which are, as previously said, present in many engineering applications. The aim of this project is therefore, to perform experiments and use the data to validate a transition model by Langtry and Menter which is expected to be a good candidate for prediction of such flows.

2 Experimental Setup

Experiments were carried out in a wind tunnel facility of Chalmers University. Tests were performed on specially designed airfoil models of large scale for obtaining thick boundary layers which enabled to conduct detailed measurements in the boundary layers. The tunnel is of open circuit blower type and was operated at velocities between 5 and 18 m/s.

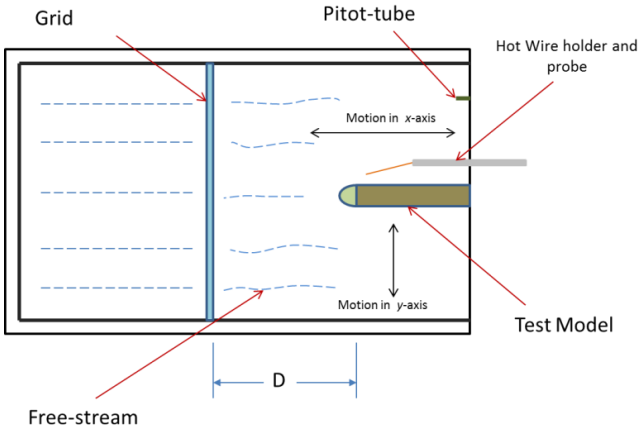

Fig. 1. Sketch of the facility test section.

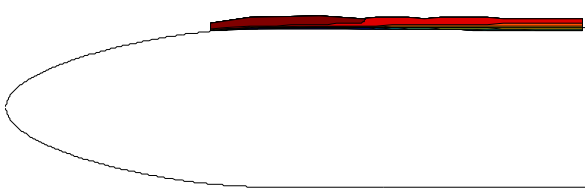

Fig. 2. Measurement region on the model.

The cross section of the facility is 200 by 1200 mm. The tunnel test section is equipped with an end-wall boundary-layer suction system for controlling the flow two-dimensionality.

Figure 1 shows a sketch of the test section of the facility. A grid is used to control the incoming flow turbulence and two turbulence intensities are procured for tests: 2% and 4%. For testing at 2% free stream turbulence intensity, the grid had to be placed at a distance, D equal to 960 mm upstream from the point where x=0 (set up of coordinates explained further in this section). The grid then is moved so that D=430 mm, which is the distance needed to get 4% free-stream turbulence intensity. Different flow velocities (5, 9 and 18 m/s) are used and the freestream velocity was monitored using a Pitot-Prandtl tube connected to a digital micro-manometer, which also had sensors for temperature and absolute pressure readings.

The measurements were done by a hot-wire anemometer. The CTA anemometer was equipped with a tungsten wire of 3 mm length and 5 μm in diameter. The probe calibration was performed in a dedicated calibrator and the maximum error in the probe calibration was within 0.5% for all calibration points. Probe positioning and data acquisition were fully automated. A three-component traversing system is controlled by stepper motors with a resolution of 1.6 μm.

The coordinate system is defined with x axis oriented in streamwise direction, y vertical and normal to the wall, and z spanwise. Preliminary tests were performed to assure the flow two-dimensionality and it was found that velocity profiles along the spanwise direction were well-uniform. The main experiments were carried at the model midspan.

Investigated nose models were attached to a flat box with their curved surfaces transformed to flat progressively. At the point of attachment, where the flat part starts, x coordinate is set to zero. This means that the streamwise coordinates along the curved surface are negative and along the flat box are positive. The 4 different leading edges were manufactured by using rapid prototyping technique. The flat part of the model is assembled by using plastic plates and aluminium profiles. Figure 3 shows the differences in shapes for the noses, and corresponding resulting pressure coefficient distributions.

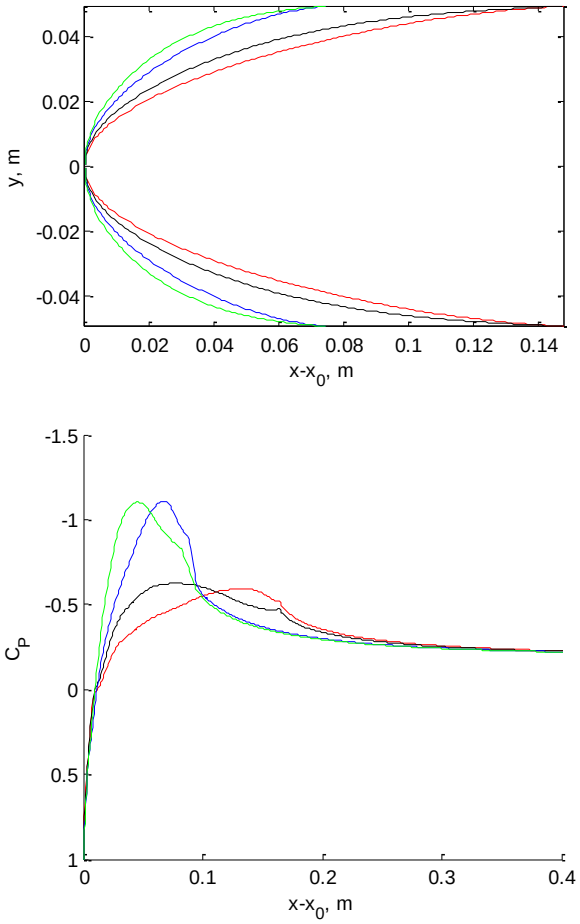

Fig. 3. Geometry of the models and corresponding pressure coefficient distributions: 95N (—), 110N (—), 95sh (—), and 110sh (—).

On every model, 15 pressure taps of 1.7 mm in diameter were designed in order to monitor the static pressure distributions. The pressures were monitored by a 16-channel PSI 9116 digital pressure scanner (Pressure System Inc.) which has a measuring range of ±2500 Pa. The accuracy of the scanner in the measurement range of current experiment (±250 Pa) is ±2 Pa.

Post-processing of the experimental data was performed in the Matlab software package by MathWorks Inc.

The experiments were performed at 3 different wind-tunnel speeds and 4 different nose geometries, which means 12 cases in total for the same free stream turbulence intensity.

For each of the 2% free stream turbulence intensity cases, 16 different locations along *x*-axis were taken for measuring and for each *x*-position, 27 points along the *y*-axis were determined, for a total of 432 spatial coordinates or measuring points, see Fig. 2.

The base configurations are two modifications of the NACA6 airfoil nose (a sharper modification and a more blunt modification). Two other models are created by decreasing twice the aspect ratio of the base configurations. Therefore, 4 different noses, for modelling of 4 different pressure gradients, were manufactured for testing. The resulting modified noses were named 95N (large-scale sharp nose), 110N (large-scale blunt nose), 95sh (short version for 95N) and 110sh (short version for 110N).

The pressure distributions for both large-scale noses (95N and 110N) and their short versions (95sh and 110sh) are shown along the streamwise coordinate x-x_0 (distance from the leading edge). From Fig. 3 it is clearly seen that the 95-noses have the location of the pressure peak shifted downstream as compared to 110-noses and the favourable pressure gradient extends up to the point of connection with the flat box. For the 110-noses the adverse pressure gradient starts already on the curved surface of the nose. The 110sh nose causes the strongest favourable pressure gradient and for three other noses the favourable pressure gradient strength is decreased in the following order: 95sh, 110N, 95N.

3 Numerical Setup

The numerical calculations were performed with Gamma-Theta transition turbulence model by Langtry and Menter [1]. This correlation-based model uses transport equations for intermittency and momentum thickness Reynolds number. The intermittency equation is coupled with Menter's $k-\omega$ SST model and used to turn on the production of the turbulent kinetic energy beyond the turbulent transition region. The second transport equation is formulated in terms of the momentum thickness Reynolds number at transition onset. An empirical correlation is used to control the transition onset criteria in the intermittency equation.

Steady two-dimensional computations were performed by using pressure based implicit finite volume solver and second-order discretization of the equations. The computational domain consisted of 10^5 quadrilateral cells with an O-grid surrounding the model with a resolved near-wall layer ($y^+<1$). Boundary conditions in the numerical calculations were carefully matched with corresponding conditions from the wind tunnel tests. At the inlet the velocity, turbulence intensity and inlet turbulent length scale were set as in the experiments.

Numerical data, as the experiments, were obtained for totally 16 flow cases with different flow Reynolds number, turbulence intensity and pressure gradient distributions.

4 Results and Discussion

Effect of flow Reynolds number (*Re*), pressure gradient and free stream turbulence intensity (*Tu*) on transitional flow were individually investigated as explained below.

4.1 Procedure of Transition Measurement

In Fig. 4 a set of profiles of mean and r.m.s. velocity are shown for case 95N at 9 m/s and 2% free stream turbulence intensity. This is a case of a mild favourable pressure gradient and medium Reynolds number. The shown profiles are from every third measured *x*-station.

From the mean velocity profiles it is clearly seen that for the mentioned case, the boundary layer is initially laminar and the profiles have shape close to the Blasius profile. The measurement point at x=-35 mm is located in the mild favourable pressure gradient and the velocity profile there demonstrates a slightly more full shape than the Blasius profile and at the measurement point x=60 mm the mild adverse pressure gradient leads to formation of a less full profile than the Blasius profile. The r.m.s. velocity distribution at the first measurement station reveals a typical shape for a laminar boundary layer subjected to a high turbulence intensity. One can observe that the

magnitude of fluctuations is increased from the freestream value of 2% up to 8% inside the boundary layer and the peak value is located in the middle of the boundary layer at y=3.5θ. The laminar-turbulent transition starts at next streamwise position, x=60 mm and proceeds down to x=120 mm. The maximum turbulence intensity of 14% can be observed in the middle of the transitional range at x=90 mm. It is seen that from this station the position of maximum r.m.s. in the boundary layer is shifted towards the wall, which is typical for a turbulent boundary layer.

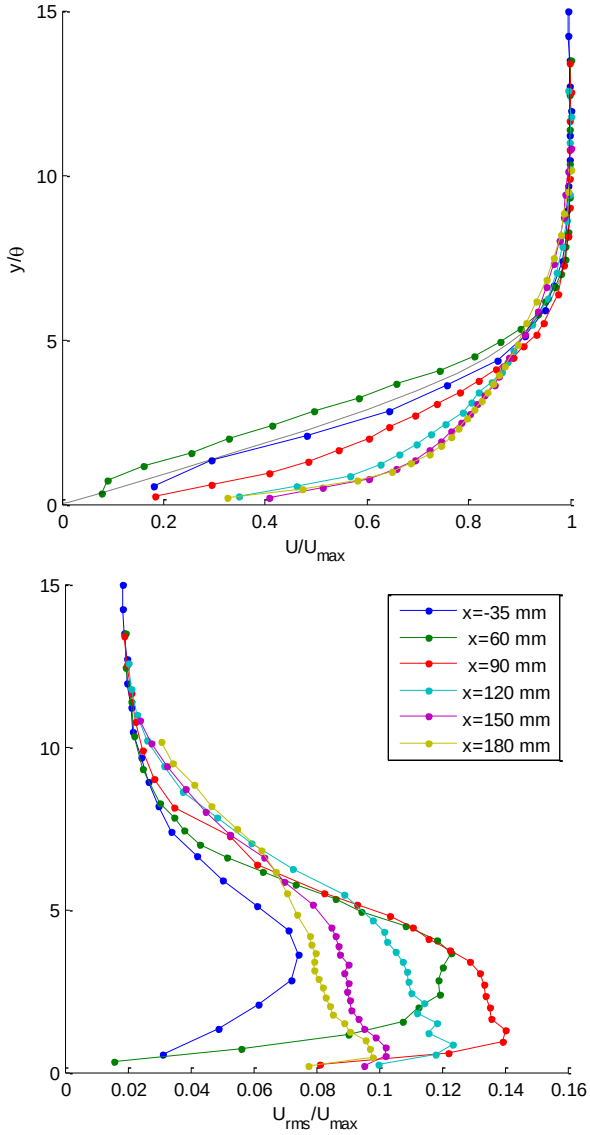

Fig. 4. Measured mean velocity (*top*) and r.m.s. (*bottom*) profiles for model 95N at 9 m/s and freestream turbulence intensity, *Tu*=2%. Dashed line depicts the Blasius mean velocity profile.

The last two measurement stations, x=150 and x=180 mm are typical for a turbulent equilibrium boundary layer with observable similarity for both the mean and r.m.s. velocity profiles.

As follows from the above discussion to identify the state of the boundary layer and the transition location one needs to analyse the shape of the mean velocity profiles. The monitoring of local turbulence intensity in a point is not sufficient for evaluation if the boundary layer is in a laminar or turbulent state. In fact, the value of local turbulence intensity in the near wall region (scaled by the local mean velocity) is higher within the laminar part of thr flow.

Typical streamwise development of velocity traces is shown in Fig. 5 for the same measurement case. One can observe that the major difference between the laminar and turbulent flow in this case is in the time-scale of the fluctuations. The long-scale fluctuations are observed in laminar region and the transitional and turbulent regions are associated with short-wavelength fluctuations with the wavelength of the order of 30θ (which corresponds to 3-4δ_{99}) and shorter. The signal which is high-pass filtered at frequency corresponding to this wavelength is shown in Fig. 6. The intermittency function determined from the high-pass filtered signal is depicted in this figure as well. As seen, using the intermittency function is very effective way of determining the transition location. Care should be taken, however, in finding the appropriate value for the filtering frequency and threshold.

In current study a complex analysis was used for the identification of transition location. The mean and r.m.s. velocity distributions were examined as well as the intermittency. The most effective way of CFD validation was found by using the comparison of the shape factor distributions. As one can observe in Fig. 7 the shape factor reflects well changes of the boundary layer state. In laminar region around the point of zero-pressure gradient the shape factor is close to the theoretical value of 2.59 for the Blasius flow and approaching value of 1.5 in the turbulent region.

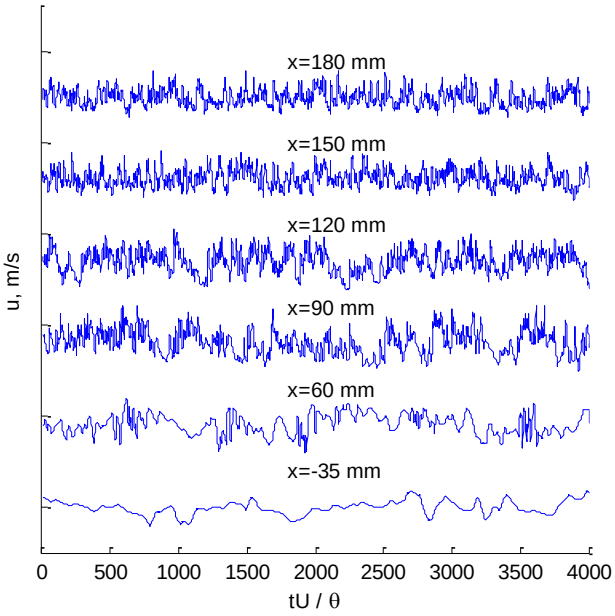

Fig. 5. Velocity traces measured at location of maximum r.m.s. in boundary layer for model 95N at 9 m/s and *Tu*=2%.

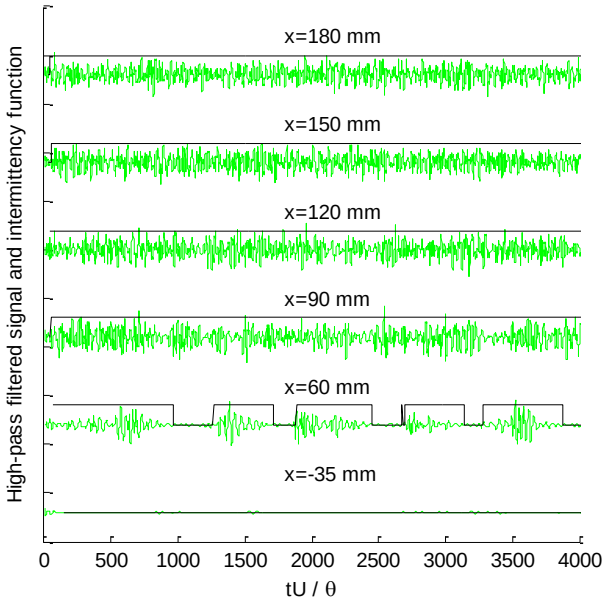

Fig. 6. High-pass filtered velocity traces and the intermittency function.

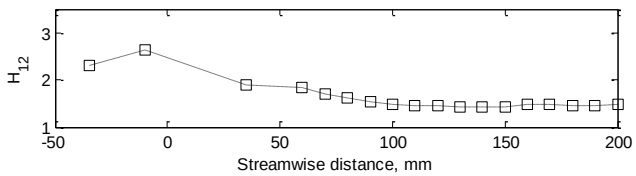

Fig. 7. Shape factor distribution for model 95N at 9 m/s and *Tu*=2%.

4.2 Effect of Reynolds Number

Figure 8 shows a contour plot of the mean velocity for the 95N case at different inflow Reynolds numbers. The velocity is scaled by the inlet velocity. It is seen that the boundary layer is gradually becoming thinner as Reynolds number increases. Figure 9 shows, for the same case, how a turbulent region moves upstream as flow Reynolds number increases. It also shows that r.m.s. amplitude is higher at higher values of *Re*. Finally, it is possible to note that the lowest flow Reynolds number produces the longest transitional region.

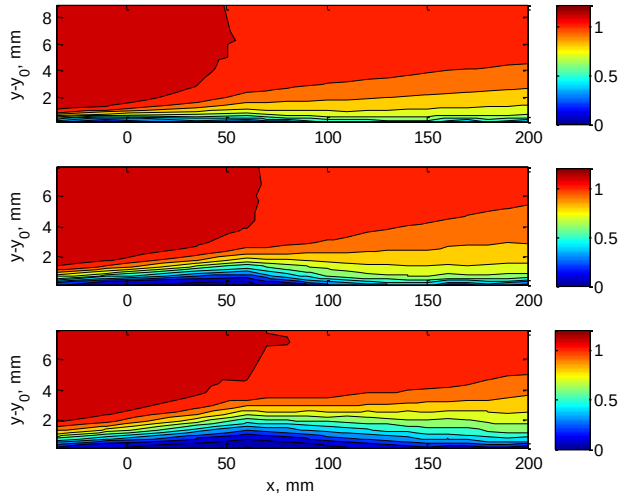

Fig. 8. Mean velocity for the 95N nose at 5, 9 and 18 m/s (from bottom top).

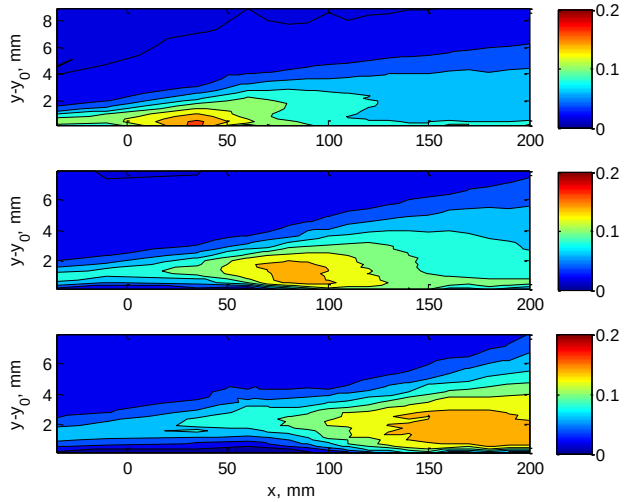

Fig. 9. R.m.s. velocity for the 95N nose at 5, 9 and 18 m/s (from bottom top).

4.3 Effect of Pressure Gradient

Contour plots in Figure 10 show turbulence intensity distributions for two cases of different pressure gradient. The top part of the figure shows measurements for the case of more aggressive pressure gradient distribution with nose 95sh and. One can observe that the transition point moves upstream when a stronger adverse pressure gradient is present. The level of maximum turbulence is also higher in that case, when compared to less strong adverse gradient case. At the same speed and free-stream turbulence level, the effect of increasing the adverse pressure gradient is, as might be expected, an earlier transition beginning. By looking at the points where the transition starts and finishes, it is seen that the length of the transitional region is also decreased in case of stronger adverse pressure gradient from 100 mm to 50 mm.

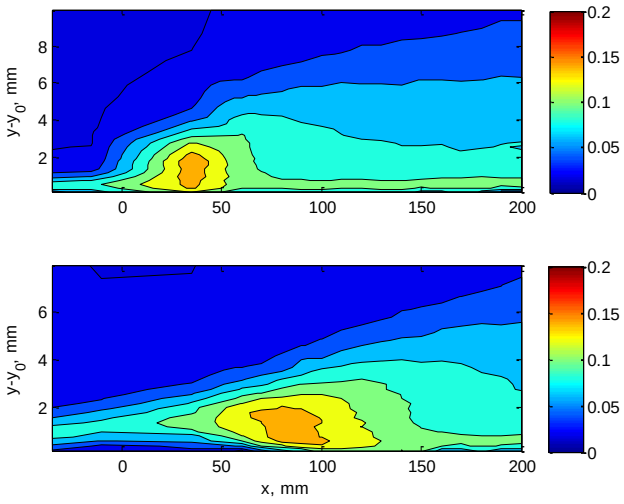

Fig. 10. Turbulence promotion by the pressure gradient (95sh top and 95N bottom). Same *Re* (velocity 9 m/s) and *Tu* = 2%.

4.4 Effect of Free-stream Turbulence Intensity

The contour plot in Figure 11 shows graphically how boundary layer turbulence varies when the free-stream turbulence is different. As it is expected, higher level of the freestream turbulence promotes the transition onset. The length of the transitional region seems to be same at higher *Tu*. It is noticeable that in the case of *Tu*=4% and highest velocity (not shown) the transition occurs already in the zone of favourable pressure gradient.

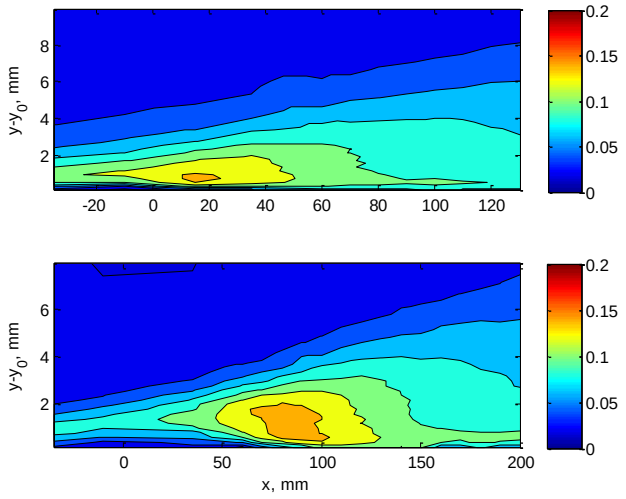

Fig. 11. Turbulence promotion by the increased turbulence intencity (4% top and 2% bottom). Same *Re* (velocity 9 m/s) and airfoil model (95N).

4.5 Comparison of CFD calculations and Experiments

It is well known that the simulation of laminar-turbulent transition is particularly challenging task for turbulence modelling. A number of turbulence models are developed which claim possibility of transition prediction and none of them is proven to be flawless so far. A relatively new transition model suggested by Langtry and Menter [1] was used in current study. These numerical calculations were performed for same geometries as in experiments and were validated by using current experiments.

Figures 12 to 14 show relevant results when CFD and experiments are compared. It is possible to see that for the mild adverse pressure gradient, the predictions are quite good at high flow velocities (Figure 12) and in the low Reynolds number range the predictions are reasonably good. Very good predictions can be observed at strong adverse pressure gradient cases (Figure 13) for all flow velocities. When the turbulence intensity is increased, the mid flow velocity and mild adverse pressure gradient case showed the best result (Figure 14).

For case *Tu*=4% and velocity of 9 m/s the transition occurs already in the zone of favourable pressure gradient. In this case the CFD is slightly under predicting the transition location. In general the CFD tends to over predict the transition location at mild adverse pressure gradients and to over-predict at strong adverse pressure gradient.

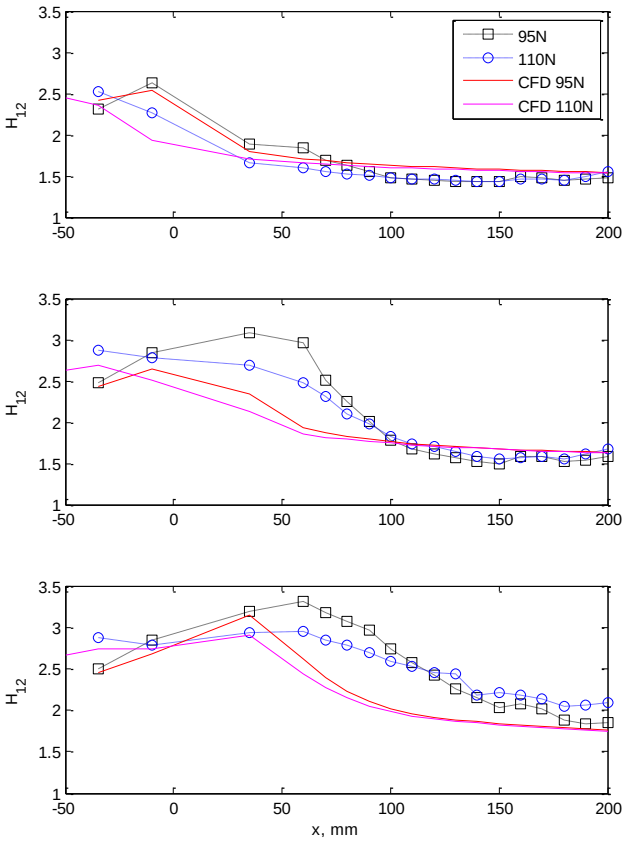

Fig. 12. Comparison of boundary layer shape factor from CFD (lines) and experiments (symbols) for airfoil models 95N and 110N at 5m/s, 9m/s and 18m/s (from bottom to top) and *Tu*=2%.

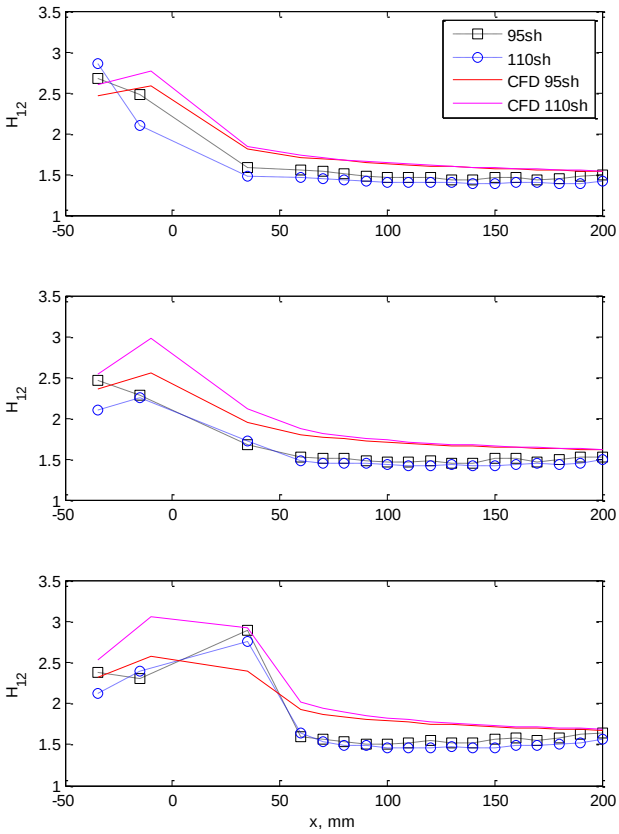

Fig. 13. Comparison of boundary layer shape factor from CFD (lines) and experiments (symbols) for airfoil models 95sh and 110sh at 5m/s, 9m/s and 18m/s (from bottom to top) and *Tu*=2%.

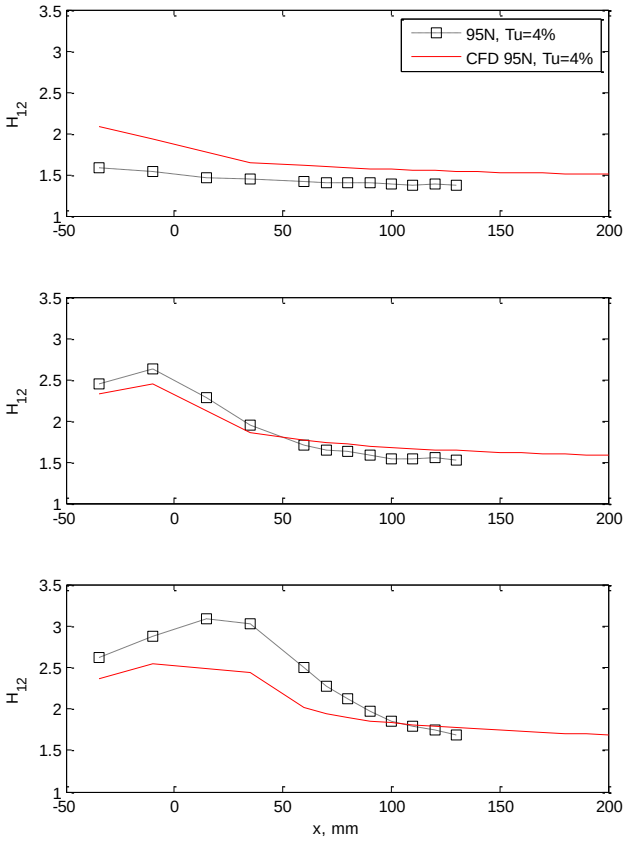

Fig. 14. Comparison of boundary layer shape factor from CFD (lines) and experiments (symbols) for airfoil model 95N at *Tu*=4% and velocities 5m/s, 9m/s and 18m/s (from bottom to top).

Conclusions

Laminar-turbulent transition at high free-stream turbulence in boundary layers of the airfoil-like geometries with presence of the external pressure gradient changeover has been studied experimentally. This study will help deepen our understanding of the transition phenomena especially for engineering applications.

The experimental data were collected for a number of flow cases with different flow Reynolds number, turbulence intensity and pressure gradient distributions. The flow parameters selected are typical for turbomachinery applications and many other engineering applications. A database for further studies and validation of numerical calculation is one of the major benefits.

The results from experiments show that the transition onset is promoted when the flow Reynolds number and the free-stream turbulence intensity are increased. This happened even when the boundary layers are subjected to strong favourable pressure gradients and adverse pressure gradients.

Numerical calculations for same geometries and flow conditions as in experiments by using SST model with transition by Langtry and Menter were tested. The numerical results are encouraging. CFD shows very good prediction of transition location for cases with strong adverse pressure gradient for both studied turbulence levels. In cases of mild adverse pressure gradient CFD computations demonstrate a reasonably good prediction with some under- or over-prediction of the transition onset.

References

[1] Menter, F.R., Langtry, R.B., Likki, S.R., Suzen, Y.B., Huang, P.G., and Völker, S., A Correlation based Transition Model using Local Variables Part 1 – Model Formulation, *ASME Paper GT2004-53452*, 2004.

[2] Langtry, R.B., Menter, F.R., Likki, S.R., Suzen, Y.B., Huang, P.G., and Völker, S., A Correlation based Transition Model using Local Variables Part 2 – Test Cases and Industrial Applications, *ASME Paper GT2004-53454*, 2004.

[3] Abu-Ghannam B.J., Shaw R. Natural Transition of Boundary Layers-The Effects of Turbulence, Pressure Gradient, and Flow History, *IMechE J.l Mech. Eng. Sci.* 22, p. 213-228, 1980.

[4] Walker G.J., Gostelow J.P. Effects of Adverse Pressure Gradients on the Nature and Length of Boundary-Layer Transition, *ASME J. of Turbomachinery*, 112, p. 196-205, 1990.

[5] Gostelow J.P., Blunden A.R. and Walker G.J. Effects of Freestream Turbulence and Adverse Pressure Gradients on Boundary-Layer Transition, *ASME J. of Turbomachinery*, 116, p. 392-404, 1994.

[6] Solomon W.J., Walker G.J. and Gostelow J.P. Transition Length Prediction for Flows with Rapidly Changing Pressure Gradients, *ASME J. of Turbomachinery*, 118, p. 744-751, 1996.

[7] Mayle R.E. The 1991 IGTI Scholar Lecture: The Role of Laminar-Turbulent Transition in Gas Turbine Engines, *ASME J. of Turbomachinery* 113, p. 509-537, 1991.

[8] Bario F., Beral C. Boundary layer measurements on the pressure and suction sides of a turbine inlet guide vane, *Exp. Thermal and Fluid Sci.* 17, p. 1-9, 1998.

[9] Van Treuren K. W., Simon T., Von Koller M., Byerley A.R., Baughn J.W., Rivir R. Measurements in a turbine cascade flow under ultra-low Reynolds number conditions, ASME J. of Turbomachinery, 124 p. 100-106, 2002.

Copyright Statement

The authors confirm that they, and/or their company or organization, hold copyright on all of the original material included in this paper. The authors also confirm that they have obtained permission, from the copyright holder of any third party material included in this paper, to publish it as part of their paper. The authors confirm that they give permission, or have obtained permission from the copyright holder of this paper, for the publication and distribution of this paper as part of the ICAS2012 proceedings or as individual off-prints from the proceedings.